Methods for correcting tilt anisoplanatism in laser-guide-star-based multiconjugate adaptive optics

Brent L. Ellerbroek and François Rigaut

Gemini Observatory, 670 North A'ohoku Place, Hilo, Hawaii 96720

Received October 19, 2000; revised manuscript received February 28, 2001; accepted April 13, 2001

Multiconjugate adaptive optics (MCAO) is a technique for correcting turbulence-induced phase distortions in three dimensions instead of two, thereby greatly expanding the corrected field of view of an adaptive optics system. This is accomplished with use of multiple deformable mirrors conjugate to distinct ranges in the atmosphere, with actuator commands computed from wave-front sensor (WFS) measurements from multiple guide stars. Laser guide stars (LGSs) must be used (at least for the forseeable future) to achieve a useful degree of sky coverage in an astronomical MCAO system. Much as a single LGS cannot be used to measure overall wave-front tilt, a constellation of multiple LGSs at a common range cannot detect tilt anisoplanatism. This error alone will significantly degrade the performance of a MCAO system based on a single tilt-only natural guide star (NGS) and multiple tilt-removed LGSs at a common altitude. We present a heuristic, low-order model for the principal source of tilt anisoplanatism that suggests four possible approaches to eliminating this defect in LGS MCAO: (i) tip/tilt measurements from multiple NGS, (ii) a solution to the LGS tilt uncertainty problem, (iii) additional higher-order WFS measurements from a single NGS, or (iv) higher-order WFS measurements from both sodium and Rayleigh LGSs at different ranges. Sample numerical results for one particular MCAO system configuration indicate that approach (ii), if feasible, would provide the highest degree of tilt anisoplanatism compensation. Approaches (i) and (iv) also provide very useful levels of performance and do not require unrealistically low levels of WFS measurement noise. For a representative set of parameters for an 8-m telescope, the additional laser power required for approach (iv) is on the order of 2 W per Rayleigh LGS.

OCIS codes: 010.1080, 010.7350.

1. INTRODUCTION

Studies of multiconjugate adaptive optics (MCAO) are becoming more widespread, comprehensive, and precise.[1–7] Methods and results are now available to quantitatively assess MCAO performance as a function of parameters, including the atmospheric turbulence profile; the number, conjugate ranges, and orders of the deformable mirrors (DMs); the number and directions of the wave-front-sensing guide stars; and wave-front sensor (WFS) measurement noise. From these results, it is clear that laser guide stars (LGSs) will be required to achieve scientifically useful levels of sky coverage for astronomical MCAO systems, except perhaps for future extremely large telescopes employing revolutionary WFSs and reconstruction algorithms.[6] However, initial studies of LGS MCAO performance have revealed a disappointing surprise: Although the corrected field-of-view (FoV) of the LGS MCAO configuration represents a useful improvement over what would be feasible with a conventional adaptive optics (AO) system employing a single DM and WFS, performance is still much poorer than is predicted for natural guide star (NGS) MCAO, particularly in terms of the spatial uniformity of the corrected point-spread function and the Strehl ratio.[2] This defect is a symptom of tilt anisoplanatism. Just as a single LGS cannot (presently) be used to measure wave-front tilt because the precise position of the laser beacon on the sky is uncertain, tilt anisoplanatism cannot be reliably measured from the apparent separation between multiple LGSs. This limitation must be overcome for LGS MCAO to achieve its full performance potential.

Fortunately, a very large fraction of tilt anisoplanatism is driven by a few modal components of the atmospheric turbulence profile that are easily visualized and measurable in several different ways. For the Kolmogorov turbulence spectrum, most tilt anisoplanatism is induced by quadratic phase screens displaced in range from the telescope aperture. The phase screen $s(x, y) = x^2$ located at range h, for example, introduces the wave-front aberration $\phi(x, y) = (x + \theta_x h)^2 = x^2 + 2\theta_x hx + (\theta_x h)^2$ for a point source at infinity in the direction (θ_x, θ_y). The term $2\theta_x hx$ is a wave-front tilt term that varies with the direction θ of the source, i.e., tilt anisoplanatism. Two additional patterns of tilt anisoplanatism correspond to the phase screen modes $s(x, y) = y^2$ and $s(x, y) = xy$. Since the amplitude of the term $2\theta_x hx$ is proportional to the range h of the phase screen, the amount of tilt anisoplanatism associated with a given three-dimensional turbulence profile can be determined from the first altitude moments of these three modes. This observation suggests several possible approaches for detecting and correcting tilt anisoplanatism in a LGS-based MCAO system:

1. Measure tilt anisoplanatism directly using multiple tip/tilt guide stars in different directions. These can be

either NGSs or perhaps LGSs if the position-uncertainty problem can somehow be solved. Only three tip/tilt guide stars are necessary, since the three dominant modes of tilt anisoplanatism vary smoothly (linearly) with field angle. The use of multiple tip/tilt guide stars to reduce tilt anisoplanatism in conventional LGS AO systems has already been suggested.[8]

2. Measure tilt anisoplanatism indirectly by reconstructing the first altitude moments of the three quadratic modes of atmospheric turbulence. We will show that differencing the quadratic wave-front measurements from guide stars at two different ranges yields useful approximations to these moments. In a MCAO system these quadratic measurements might be obtained from either a single NGS and multiple sodium LGS or perhaps from multiple sodium LGS and multiple Rayleigh LGS.

In Section 2 we discuss this simple model for the origins of tilt anisoplanatism and consider its consequences in somewhat greater detail. Section 3 contains sample numerical results to test some of the predictions of the heuristic model. These calculations use analytical methods described previously[2] and are based upon AO system and scenario parameters related to, but not identical with, the MCAO configuration proposed for the Southern 8-m Gemini Telescope at Cerro Pachon. The results include the effects of the full Kolmogorov turbulence spectrum and wave-front fitting error due to the finite spatial resolution of DMs and WFSs. All of the approaches listed above for compensating tilt anisoplanatism bring the performance of a LGS-based MCAO system closer to NGS MCAO, although using higher-order measurements from a NGS WFS provides only a moderate improvement for this sample problem. The remaining possibilities compensate for at least 80% of the Strehl ratio penalty due to tilt anisoplanatism.

Section 4 considers the effect of WFS measurement noise upon three of the approaches suggested for correcting tilt anisoplanatism. The NGS signal levels required for either multiple tip/tilt NGS WFS or a single higher-order NGS WFS appear to be reasonable, but quantitative sky coverage estimates are beyond the scope of this analysis. Laser-power requirements for Rayleigh LGS are considered in somewhat greater detail. For one representative set of system parameters, the required laser power is on the order of 2 W per beacon for 2-m subapertures, a 15-km LGS range, and a 250-meter LGS range gate.

Section 5 is a brief conclusion. Finally, the authors wish to acknowledge the related work of David Fried, who we believe was the first to recognize that tilt anisoplanatism could be accurately determined from tip/tilt measurements from three NGSs.[8]

2. MOTIVATION FOR THE METHODS

In this section we study a simple "toy problem" to gain intuition as to why the methods proposed in this paper for correcting tilt anisoplanatism in LGS-based MCAO systems might be expected to work. For this purpose, consider a two-dimensional layered atmospheric turbulence profile, with each phase screen $s_i(x)$ at range h_i consisting of only linear and quadratic terms:

$$s_i(x) = a_i x + b_i x^2. \tag{1}$$

Using a paraxial ray-trace model for light propagating through the atmosphere, the turbulence-induced phase distortion $\phi(x;\ \theta,\ H)$ that is accumulated for a point source in direction θ at range H is described by the formula

$$\begin{aligned}\phi(x;\ \theta,\ H) &= \sum_{h_i<H} s_i\left[\theta h_i + \left(1 - \frac{h_i}{H}\right)x\right] \\ &= a(\theta,\ H)x + b(\theta,\ H)x^2 + c(\theta,\ H).\end{aligned} \tag{2}$$

Here the coefficients $a(\theta,\ H)$ and $b(\theta,\ H)$ of the linear and quadratic terms of the wave front are defined by

$$a(\theta,\ H) = \sum_{h_i<H}\left(1 - \frac{h_i}{H}\right)(a_i + 2\theta h_i b_i), \tag{3}$$

$$b(\theta,\ H) = \sum_{h_i<H}\left(1 - \frac{h_i}{H}\right)^2 b_i, \tag{4}$$

and $c(\theta,\ H)$ is the piston term of the wave front, which is of no particular interest. In the special case of a source at infinity the coefficients $a(\theta,\ \infty)$ and $b(\theta,\ \infty)$ may be written as

$$a(\theta,\ \infty) = \mu_0(a) + 2\theta\mu_1(b), \tag{5}$$

$$b(\theta,\ \infty) = \mu_0(b), \tag{6}$$

where the nth moment of the sequence $\{x_i\}$ is defined by the expression

$$\mu_n(x) = \sum_i h_i^n x_i. \tag{7}$$

From Eq. (5) we see that the wave-front tilt errors induced by atmospheric turbulence are the sum of a global tilt term proportional to $\mu_0(a)$ and an anisoplanatic term proportional to $\mu_1(b)$. Higher-order aberrations in a real atmosphere will contribute additional tilt errors, but for a Kolmogorov turbulence spectrum these two terms will remain the dominant modes, provided that the beam displacements $h_i\theta$ are small compared with R, the radius of the telescope aperture. Appendix A computes the relative contributions to tilt anisoplanatism due to the second- and third-order Zernike components of atmospheric turbulence for a Kolmogorov turbulence spectrum.

In a conventional LGS AO system, a single LGS is projected at range H in the direction θ of the science object of interest. In the vocabulary of this toy problem the LGS provides a measurement of the higher-order wave-front aberration $b(\theta,\ H)$, but the wave-front tilt term $a(\theta,\ H)$ cannot be measured, owing to the position uncertainty of LGSs. A nearby NGS is required to measure the tip/tilt term $a(\theta',\ \infty)$ with $\theta' \approx \theta$. The level of atmospheric turbulence compensation feasible with this approach depends on the wave-front errors due to the cone effect and tilt anisoplanatism, i.e. the differences $b(\theta,\ \infty) - b(\theta,\ H)$ and $a(\theta,\ \infty) - a(\theta',\ \infty)$.

The purpose of a MCAO system is to compensate turbulence-induced phase errors, and in particular wave-front tilt, over an extended field-of-view (FoV). From Eq. (5), this goal can only be achieved if the global tilt term $\mu_0(a)$ and the tilt anisoplanatism term $\mu_1(b)$ can be separately estimated and corrected. This does not appear to be possible if the guide star constellation consists of only a single tip/tilt NGS and multiple tilt-removed LGSs at a single altitude. According to Eq. (4) all of the LGSs provide identical approximate measurements of the turbulence-induced focus error $\mu_0(b)$, and a single NGS tip/tilt measurement is the sum of contributions from global tilt and tilt anisoplanatism that cannot be disentangled. Clearly, these limitations will not be removed when a three-dimensional atmosphere and the full spectrum of atmospheric turbulence are included in the analysis, even if (as is the case), the cubic and higher modes of the turbulence can be accurately estimated with use of multiple LGSs.

There are, however, at least three potential methods for correcting tilt anisoplanatism in LGS-based MCAO systems if the guide-star constellation and set of WFS measurements are increased beyond the inadequate starting point of a single tip/tilt NGS and multiple tilt-removed LGS at a single altitude. Heuristic descriptions of these approaches are given below, to be followed by quantitative performance estimates in Section 3:

Multiple tip/tilt NGS. Tip/tilt measurements from multiple NGSs can detect tilt anisoplanatism almost by definition. With tip/tilt guide stars in direction θ and $-\theta$, for example, the value of the global tilt and tilt anisoplanism modes can be determined with use of the formulas

$$\mu_0(a) = [a(\theta, \infty) + a(-\theta, \infty)]/2, \tag{8}$$

$$\mu_1(b) = [a(\theta, \infty) - a(-\theta, \infty)]/(4\theta). \tag{9}$$

At least three tip/tilt guide stars are necessary with a three-dimensional atmosphere, since three different patterns of tilt anisoplanatism are introduced by the first moments of the focus and astigmatic components of the phase screens.

Solving the LGS tilt-uncertainty problem. If the LGS tilt mode $a(\theta, H)$ were measurable it could be substituted into Eqs. (8) and (9) above to obtain an estimate of the moments $\mu_0(a)$ and $\mu_1(b)$. This estimate would be only approximate owing to the cone effect, and a single tip/tilt NGS might still be desirable for an improved estimate of global tilt.

Quadratic wave-front measurements at multiple altitudes. Heuristically, the moment $\mu_1(b)$ is driven by the quadratic components of the phase screens at upper altitudes. Differencing the quadratic measurements from guide stars at different ranges might be expected to identify these terms. Using Eq. (4), we can write the difference between the quadratic measurements from guide stars at two different altitudes H_1 and H_2 with $H_1 \leqslant H_2$ as

$$b(\theta, H_2) - b(\theta', H_1) = 2(H_1^{-1} - H_2^{-1})\mu_1(b) + \sum_i f_i b_i, \tag{10}$$

where the coefficients f_i of the error term are given by

$$f_i = \begin{cases} h_i^2(H_2^{-2} - H_1^{-2}) & \text{if } h_i \leqslant H_1 \\ 1 - 2h_i H_1^{-1} + h_i^2 H_2^{-2} & \text{if } H_1 \leqslant h_i \leqslant H_2 \\ 2h_i(H_2^{-1} - H_1^{-1}) & \text{otherwise} \end{cases}. \tag{11}$$

Note that differencing the two quadratic measurements does not yield an abrupt, binary weighting of the upper altitude turbulence but a smooth weighting on account of the differential cone effect associated with the two guide-star ranges.

In a sodium-guide-star-based MCAO system, there may be two ways to obtain quadratic wave-front measurements at a second range. The first is to use NGSs for both tip/tilt and quadratic measurements. In this case $H_2 = \infty$ and $H_1 \approx 90$ km, the mean range to the sodium layer. The second method is to use Rayleigh guide stars at a much lower altitude, so that $H_2 \approx 90$ km and $H_1 \leqslant 20$ km. For us to estimate the moment $\mu_1(b)$ accurately with use of Eq. (10), the two altitudes should be such that (i) the measurement sensitivity coefficient

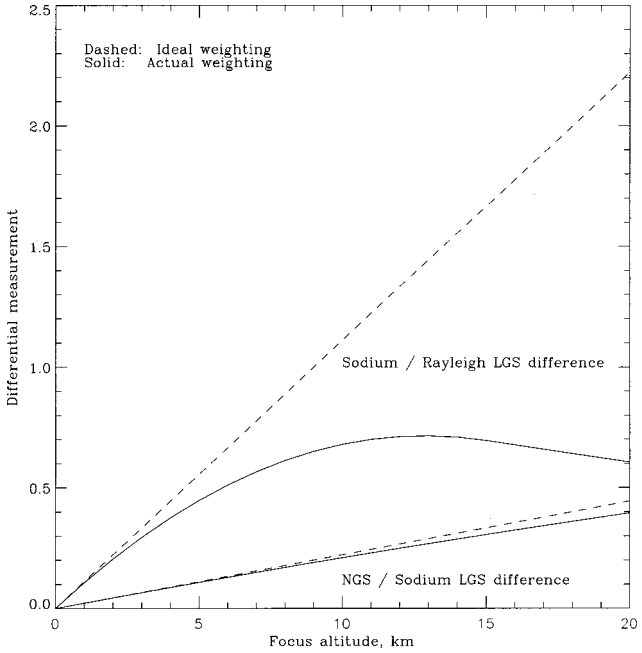

Fig. 1. Altitude weighting of atmospheric focus aberrations for a differential focus measurement between a pair of guide stars at different altitudes. Owing to the cone effect, the first altitude moment of the focus component of atmospheric turbulence, $\mu_1(b)$, may be estimated by differencing the focus terms of the wave-front measurements from a pair of guide stars at two different ranges. This figure plots the value of the differential focus measurement $b(\theta, H_1) - b(\theta', H_2)$ as a function of the altitude h of a single-layer focus aberration of unit amplitude. The lower solid curve is for the guide-star ranges $H_1 = 90$ km and $H_2 = \infty$, and the upper solid curve corresponds to the case $H_1 = 15$ km, $H_2 = 90$ km. The dashed curves describe linear approximations $2(H_1^{-1} - H_2^{-1})h$. If the difference between this linear approximation and the actual value of $b(\theta, H_1) - b(\theta', H_2)$ is small, the focus moment $\mu_1(b)$ may be estimated as $[b(\theta, H_2) - b(\theta', H_1)][2(H_1^{-1} - H_2^{-1})]^{-1}$ with acceptable accuracy, independently of the vertical distribution of the atmospheric turbulence layers. If the slope of the linear approximation is large, this estimate will be more robust with respect to WFS measurement noise and the spatial aliasing of higher-order wave-front modes.

$2(H_1^{-1} - H_2^{-1})$ appearing on the right-hand side of this equation is large, and (ii) the coefficients f_i of the error term are comparatively small. The first condition implies reduced sensitivity to WFS measurement noise and spatial aliasing from higher-order wave-front aberrations. With the second condition, the moment $\mu_1(b)$ can be estimated as $[b(\theta, H_2) - b(\theta', H_1)][2(H_1^{-1} - H_2^{-1})]^{-1}$ with acceptable accuracy, independently of the vertical distribution of the turbulence layers.

Figure 1 plots the differential focus measurement $b(\theta, H_2) - b(\theta', H_1)$ computed from Eq. (10) as a function of the altitude h of a single-focus aberration with unit amplitude. The pairs of guide-star altitudes considered are (a) $H_1 = 90$ km, $H_2 = \infty$, and (b) $H_1 = 15$ km, $H_2 = 90$ km. Figure 1 also plots the function $2(H_1^{-1} - H_2^{-1})h$ [i.e., the linear term on the right-hand side of Eq. (10)] for the same two pairs of guide-star altitudes. The difference between this linear function and the actual value of $b(\theta, H_2) - b(\theta', H_1)$ is equal to the nonlinear error term in Eq. (10). Figure 1 suggests that it may be difficult to maximize the sensitivity coefficent $2(H_1^{-1} - H_2^{-1})$ and simultaneously minimize the magnitude of the nonlinear error term: The error term is much smaller for the sodium LGS and NGS combination, but the sensitivity of the Rayleigh/sodium LGS combination is much higher. It appears that the comparative performance of the two methods must be evaluated with use of more sophisticated analytical methods, as is illustrated in Section 3 for one particular sample problem.

3. SAMPLE NUMERICAL RESULTS

This section presents a limited selection of sample numerical results to illustrate the performance of the various methods described above for compensating tilt anisoplanatism in a LGS-based MCAO system. These calculations demonstrate the importance of correcting tilt anisoplanatism for MCAO and begin to assess the potential performance of the different approaches suggested in Section 2. The principal implementation issue studied in this analysis is the spatial aliasing of higher-order wave-front modes into the quadratic wave-front measurements used to estimate tilt anisoplanatism. The effect of WFS measurement noise is investigated below in Section 4.

All calculations presented in this section are for an aperture diameter D of 8 m, the median Cerro Pachon turbulence profile,[9] an evaluation wavelength of 2.2 μm, and higher-order WFSs and DMs of order 12×12. Table 1 lists the altitudes and weights for the seven-layer discretization of the turbulence profile. We have used a Kolmogorov turbulence spectrum with an infinite outer scale and a Fried parameter r_0 of 0.166 meters at λ=0.5 μm. This corresponds to $D/r_0 = 8.14$ at the evaluation wavelength. The isoplanatic angle is 2.74 arc sec at 0.5 μm and 16.2 arc sec at 2.2 μm. All calculations are also for the case of five higher-order Shack–Hartmann WFSs observing guide stars located at the center and corners of a 68.7 arc sec square FoV and three zonal deformable mirrors optically conjugate to ranges of 0, 4, and 8 km. The orders of the three DMs are 12, 12, and 6 interactuator spacings across an 8-m beam diameter, and the FoV half-width corresponds to a beam shear of one actuator spacing at both the second and third DM.

The analytical methods used for these calculations have been described previously.[2] The usual linear systems model based upon geometric optics approximations is used to model the turbulence-induced phase distortions, the wave-front gradient measurements obtained from tip/tilt sensors and Shack–Hartmann wave-front sensors, and the wave-front corrections applied by the zonal deformable mirrors. The so-called minimal variance wave-front reconstruction algorithm is derived from atmospheric turbulence statistics and the DM-to-WFS influence matrix to minimize the aperture- and field-averaged variance of the residual phase error after AO compensation. This optimization is subject to a constraint that improves loop stability and greatly simplifies performance evaluation for a closed-loop servo system, although servo lag effects have not been included in this study. The effects of WFS measurement noise are likewise neglected in this section but will be considered later. Note that minimizing the field-averaged phase variance with use of this algorithm does not necessarily yield the most uniform correction of the turbulence across the FoV, and that somewhat more uniform Strehl ratios can be achieved at the expense of a slightly lower mean value.

Using the above model, we may express the second-order statistics of the residual wave-front errors left uncorrected by the AO system in terms of the atmospheric turbulence parameters, WFS subaperture geometries and noise levels, DM actuator geometries and conjugate ranges, and the AO control-loop bandwidth.[2] These expressions for the wave-front error statistics are subject to numerical evaluation, and the Strehl ratios achieved by the AO system may then be computed if we are willing to assume that these errors are normally distributed. Table 2 summarizes the noise-free results computed for the sample problem considered here. AO system performance is characterized in terms of the Strehl ratio at 2.2 μm at the center, edge, and corner of the square field. Each row of the table lists system performance for a particular combination of natural, sodium, and Rayleigh guide stars, and the table is divided into subsections corresponding to the different approaches for compensating tilt anisoplanatism.

Line 1 describes the performance of a conventional NGS AO system with a single WFS and DM and a recon-

Table 1. Cerro Pachon $C_n^2(h)$ Profile for Sample Calculations[a]

Layer	h (m)	Fractional C_n^2
1	0	0.646
2	1800	0.078
3	3300	0.119
4	5800	0.035
5	7400	0.025
6	13100	0.080
7	15800	0.015

[a] This profile is a discretized fit to median $C_n^2(h)$ measurements at Cerro Pachon. h is the altitude above the site. The value of r_0 is 0.166 m at 0.5 μm, and the value of θ_0 is 2.74 arc sec.

Table 2. Sample Results for MCAO Systems with a 68.72 arc sec FoV[a]

NGS		Sodium LGS		Rayleigh LGS		Strehls at 2.2 μm		
N_n	O_n	N_s	O_s	N_r	O_r	Center	Edge	Corner
1	12					0.842	0.083	0.041
5	12					0.835	0.739	0.744
1	1	5	12			0.764	0.447	0.355
4	1	5	12			0.808	0.704	0.660
		5	12**			0.765	0.676	0.678
1	1	5	12**			0.815	0.720	0.717
1	2	5	12			0.796	0.604	0.522
1	4	5	12			0.820	0.650	0.573
1	6	5	12			0.823	0.673	0.588
1	1	5	12	5	2	0.813	0.679	0.634
1	1	5	12	5	4	0.818	0.707	0.642
1	1	5	12	5	6	0.821	0.716	0.645

[a] This table summarizes the performance of sample MCAO configurations for an 8-m telescope, the median Cerro Pachon turbulence profile, deformable mirrors conjugate to ranges of 0, 4, and 8 km, and a 68.72 arc sec square field of view. The asterisks in rows 5 and 6 indicate that the sodium LGS measurements are not tilt removed. N_n, N_s, and N_r are the number of natural, sodium, and Rayleigh guide stars. O_n, O_s, and O_r are the linear orders of the corresponding wave front sensors.

struction matrix selected to optimize on-axis performance. The on-axis Strehl ratio of 0.842 indicates the effect of fitting error, and the Strehls of 0.083 and 0.041 at the edges and corners of the field quantify the impact of anisoplanatism without MCAO.

Line 2 outlines the results achieved with a NGS MCAO system of five guide stars. Quite-uniform performance is achieved over the entire FoV, with all Strehl ratios falling between 0.744 and 0.835. Unfortunately, the sky coverage corresponding to five bright NGS within a 68 arc min square FoV can be treated as zero, and LGSs are necessary to implement MCAO on 8-m class telescopes.

In line 3, the five higher-order NGSs are replaced by five tilt-removed sodium LGSs and a single tip/tilt NGS located at the center of the FoV. The Strehl ratio at the corners of the field is reduced by more than a factor of two from 0.744 to 0.355, indicating the considerable importance of correcting tilt anisoplanatism in an LGS-based MCAO system.

Line 4 augments the sodium LGS MCAO system with four tip/tilt NGSs located at the four edges of the FoV. (Very similar results can be achieved with only three tip/tilt NGSs, but the use of four NGSs yields symmetric results that are consistent with the format of the table.) About 80% of the Strehl ratio reduction at the corner of the FoV is regained, although it should be noted that this is for the case of zero NGS WFS measurement noise. Quantitative sky-coverage calculations for this approach are complicated by the use of multiple tip/tilt NGSs and are beyond the scope of this study.

Lines 5 and 6 describe the performance, which could theoretically be achieved by solving the LGS position-uncertainty problem. It may not be surprising that nearly all the performance of the ideal NGS MCAO system is retained, particularly when a single tip/tilt NGS is included in the system to remove the tip/tilt error due to the cone effect. If any is needed, these results provide further incentive for solving this very difficult problem.

Lines 7 through 9 illustrate the level of improvement achieved when a single higher-order NGS WFS of order 2×2, 4×4, or 6×6 is included in the MCAO guide-star constellation. This approach is less successful than the others for the sample problem considered here, probably because the difference between the quadratic modes of the NGS and sodium LGS measurements is such a weak function of tilt anisoplanatism.

Lines 10 through 12 summarize MCAO performance when Rayleigh guide stars with relatively low-order wave-front sensors are included in the MCAO constellation. For simplicity we have placed the five Rayleigh LGSs in the same locations in the sky as the five sodium LGSs. The Rayleigh LGS range is 15 km. Performance is comparable with the multi-NGS system (line 4 of Table 2) to within a few percent, and sky coverage will be superior owing to the requirement for only a single tip/tilt NGS. For this reason it may be worth investigating the feasibility of this hybrid NGS/LGS MCAO approach in greater detail.

Finally, we note in passing that similar calculations have been performed for (i) a FoV width of 55.0 arc sec and DMs conjugate to ranges of 0, 5, and 10 km, and (ii) a von Karman turbulence profile with an outer scale of 30 m. The results obtained are entirely similar to the case presented in Table 1.

4. MEASUREMENT NOISE EFFECTS

A detailed study of how WFS measurement noise impacts the above results would require fairly rigorous modeling of specific WFS concepts and is beyond the scope of this paper. Still, a few very preliminary calculations are probably useful to assess whether the proposed approaches for compensating tilt anisoplanatism are at all feasible for 8-m astronomical telescopes. We restrict our attention to the sample problem considered in Section 3, and consider the case of tip/tilt sensors and Shack–Hartmann wave-front sensors implemented with use of quadrant detectors. We also assume a visible wave-front-sensing wavelength. This implies that r_0 at the sensing wavelength is much smaller than the DM interactuator spacing for our sample problem, so that the measurement sensitivity of the tip/tilt and Shack–Hartmann sensors is approximately the same as for the seeing-limited case. We evaluate the impact of WFS measurement noise for three particular guide-star configurations:

1. Five higher-order sodium LGSs and four tip/tilt-only NGSs (line 4 of Table 2);
2. Five higher-order sodium LGSs and one NGS WFS of order 4×4 (line 8);
3. Five higher-order sodium LGS, five Rayleigh LGS WFS of order 4×4, and one tip/tilt-only NGS (line 11).

We have investigated the impact of noise in the auxilliary WFS measurements for each system, since all three configurations share common characteristics in terms of sodium LGSs. All three approaches are evaluated for one-axis, one-sigma WFS tilt-measurement errors from 0 to

0.1 arc sec, but this should not be misinterpreted in any way as a level comparison between the three techniques. For example, the actual tilt-measurement errors for a given NGS will be different for approaches 1 and 2 and the effect of NGS tip/tilt measurement noise for approach 3 has not been investigated.

The results obtained for a MCAO system with five sodium LGS and four tip/tilt-only NGS are summarized in Fig. 2. This figure plots the Strehl ratio at 2.2 μm at the center, edge, and corner of the 68.7 arc sec FoV as a function of the NGS WFS tilt-measurement error. The limiting noise level for this approach is arguably ~0.05 arc sec, at which point the Strehl at the center of the field has fallen to ~46% of the ideal noise-free value. The corresponding value at the corner of the field is ~38%.

A detailed analysis of the associated NGS magnitude limit and sky coverage depends upon many design parameters that are beyond the scope of this paper, but it may be useful to roughly estimate the NGS WFS signal level that corresponds to a 0.05 arc sec tilt-measurement error. The measurement error due to noise for a quadrant detector tip/tilt sensor is a function of the signal-to-noise ratio (SNR) and the width of the short-exposure guide star image.[10] Under seeing-limited conditions, a reasonable estimate of the error for a NGS is given by the formula

$$\sigma_\theta = \frac{0.57(\lambda/r_0)}{\mathrm{SNR}}, \tag{12}$$

where σ_θ is the one-axis, one-sigma tilt measurement error; λ is the sensing wavelength; r_0 is the turbulence-induced effective coherence diameter at this wavelength; and SNR is the signal-to-noise ratio. For the representative parameters $\lambda = 0.7$ μm and $r_0 = 0.166\ \mathrm{m} \times (0.7/0.5)^{1.2} = 0.25$ m, a SNR of about 6.6 yields a tilt-measurement error of 0.05 arc sec. The required signal level is $6.6^2 = 43$ photodetection events when background noise and detector read noise are neglected, which is small enough to suggest that reasonable levels of sky coverage may be possible through use of this approach. Nothing beyond this qualitative conclusion should be deduced from this calculation, since many additional factors (sky background, telescope windshake, partial correction of the guide-star image, etc.) must be considered for a rigorous sky-coverage estimate.

Figure 3 presents equivalent results for a MCAO configuration, including five sodium LGS WFSs and one NGS WFS with 4×4 subapertures. In this case the limiting noise level corresponding to a 50% reduction in Strehl is ~0.08 arc sec. Proceeding as above, the corresponding subaperture SNR is ~4.1, and the required number of photodetection events per subaperture is ~17. Since the width of a subaperture is 2 m, the equivalent number of photodetection events for the full aperture is about 210 per measurement. This signal level is significantly greater than was computed above for the case of four tip/tilt NGSs, but further analysis of magnitude limits, sky coverage, and the relative performance of these methods for other observing scenarios is beyond the scope of this study.

Finally, Fig. 4 illustrates results for a MCAO configuration of five sodium LGS WFSs, one tip/tilt NGS WFS, and five Rayleigh LGS WFSs with 4×4 subapertures. In this case performance is a fairly weak function of the Rayleigh LGS WFS measurement error, with an error of 0.05 arc sec yielding a Strehl ratio reduction of about 0.91 at the corner of the FoV. An error of 0.1 arc sec corresponds to a reduction of about 0.79. A direct comparison with

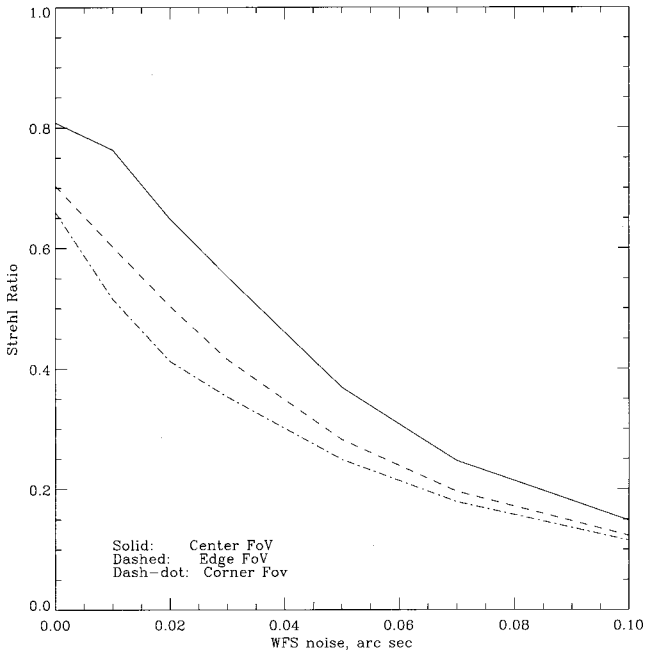

Fig. 2. Strehl versus NGS WFS noise for a MCAO system with five sodium LGS and four tip/tilt NGS WFS. These results correspond to the MCAO system parameters, the field-of-view, and the atmospheric turbulence profile of row 4 of Table 2. WFS measurement noise is expressed as a one-axis, one-sigma value.

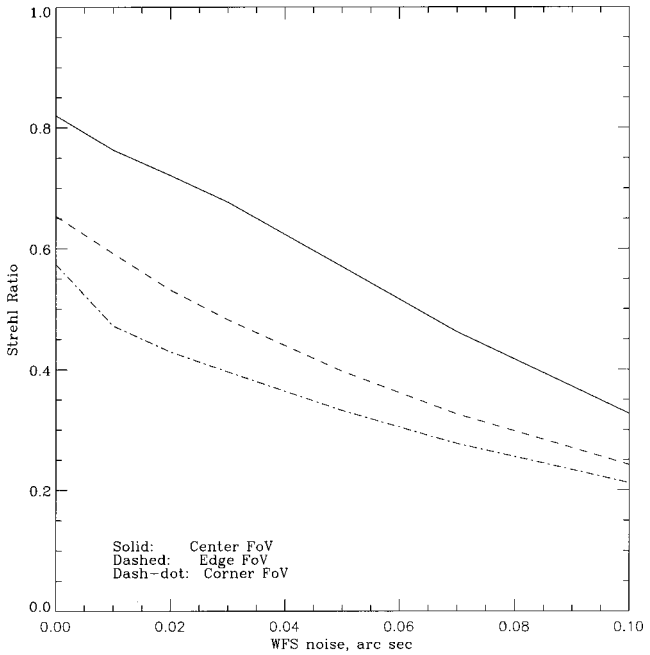

Fig. 3. Strehl versus NGS WFS measurement noise for a system with five sodium LGS and one high-order NGS WFS. This figure is analogous to Fig. 2, except that the MCAO system parameters correspond to line 8 of Table 2. The order of the NGS WFS is 4×4 subapertures.

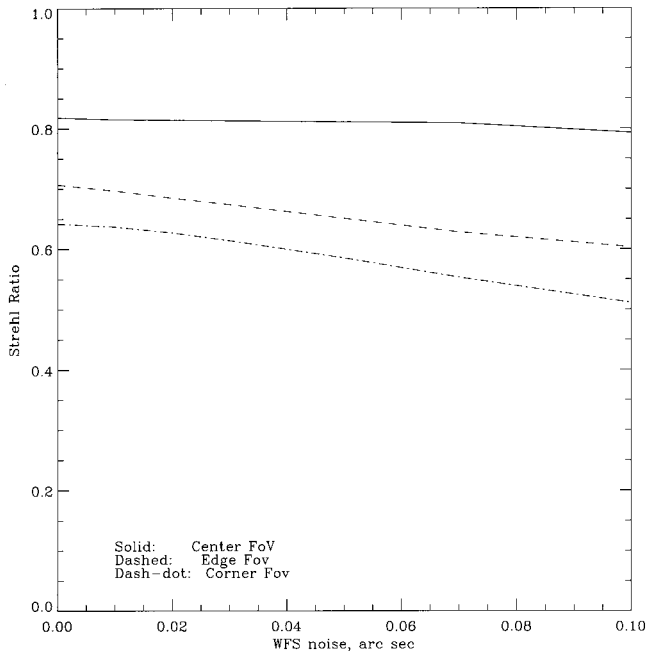

Fig. 4. Strehl versus Rayleigh WFS measurement noise for a system with five sodium LGSs and five Raleigh LGSs. This figure is analogus to Fig. 3, except that the MCAO system parameters correspond to line 11 of Table 2. The order of the Rayleigh LGS WFSs is 4×4 subapertures, and the range of the Rayleigh beacons is 15 km.

Figs. 2 and 3 would be misleading, since the WFS measurement noise is associated with the Rayleigh LGSs instead of the tip/tilt NGS. The Strehl ratio at the center of the field is a very weak function of the noise level in the Rayleigh LGS WFS, because the on-axis NGS WFS is noise free.

For a check on the feasibility of this last approach, we model the tilt-measurement error for a Rayleigh LGS using a range-gated, pulsed laser by the formula

$$\sigma_\theta = \theta_B/\mathrm{SNR}, \tag{13}$$

where θ_B is the effective angular diameter of the Rayleigh LGS image in the WFS focal plane. Formulas for evaluating this image as a convolution of transfer functions associated with different sources of blurring have been presented previously[10] but in analogy with Eq. (12) an initial estimate of θ_B can be computed as 0.57 times the root-sum-square of five contributions:

- The diffraction-limited beacon size, λ/d_T,
- Diffraction effects on the upward propagation path, λ/r_0,
- Diffraction effects on the downward path, again λ/r_0,
- Spot size of the rms due to perspective elongation, $S\,\delta z/(\sqrt{3}z^2)$,
- The rms geometric beacon size averaged over the range gate, $(\delta z d_T)/(2\sqrt{3}z^2)$.

Here λ is the guide-star wavelength (taken as 0.589 μm), d_T is the launch telescope diameter (0.3 m), δz is the length of the range gate (250 m), z is the guide-star range (15,000 m), and S is the separation from the launch telescope to the WFS subaperture (4 m). These parameters yield values of θ_B of 0.55 and 0.61 arc see, respectively, for the transfer-function-based calculation and the simpler root-sum-square-based estimate. We note that the narrow range gate of 250 m is essential for obtaining an acceptable spot size. This value is incompatible with the pulse formats of existing concepts for sodium guide-star lasers, so that separate lasers are probably necessary to generate these Rayleigh beacons.

To compute the SNR in Eq. (13), the signal level for the Rayleigh LGS WFS can be estimated with use of the equations

$$N_{\mathrm{pde}} = N_p \tau_t (\tau_a)^2 \tau_r \eta (\zeta_0 \delta z) \exp[-(z + z_o)/z_0] A_s/(4\pi z^2) \tag{14}$$

$$N_p = \left(\frac{P}{n}\right)\left(\frac{\lambda}{hc}\right). \tag{15}$$

Here, N_{pde} is the WFS signal level in photodetection events per subaperture per measurement, N_p is the number of laser photons per pulse, τ_t is the optical transmittance for the launch telescope (0.7), τ_a is the atmospheric transmittance to the guide-star range (0.8), τ_r is the optical transmittance for the Rayleigh LGS WFS optical path (0.5), η is the detector quantum efficiency (0.85), ζ_0 is the Rayleigh optical depth at sea level ($1.34 \times 10^{-5}\,\mathrm{m}^{-1}$), z_o is the altitude of the observatory (2000 meters), z_0 is the atmospheric scale height (4300 meters), A_s is the area of a subaperture (4 m^2), P is the average laser power (2 W), n is the laser pulse rate (800 Hz), and $\lambda/(hc)$ is the energy per photon. These values yield the result

$$N_{\mathrm{pde}} = 130. \tag{16}$$

The corresponding SNR is about 11 with zero read noise, and approximately 8.5 with 5 read-noise electrons per pixel per read. According to Eq. (13) the associated tilt measurement error is in the range of 0.05–0.07 arc sec.

These first-order calculations suggest that laser power should not be an issue for the Rayleigh LGS WFS measurements, especially since the wavelength could be adjusted to 0.532 μm to allow the use of solid-state Nd:YAG lasers. Servo filtering by the AO control system will also attenuate the effect of WFS measurement noise, and laser power levels somewhat greater than 2 W can certainly be considered.

5. CONCLUSION

Tilt anisoplanatism is a significant wave-front error source for a MCAO system incorporating one tip/tilt NGS and any number of tilt-removed LGSs at a common altitude. Heuristically, tilt anisoplanatism cannot be corrected with this guide-star configuration, because the altitude distribution of quadratic aberrations, specifically their first altitude moments, cannot be determined. There are four methods of measuring these moments and thereby compensating tilt anisoplanatism in a sodium-LGS-based MCAO system: (i) measure tilt anisoplanatism directly using multiple tip/tilt NGS, (ii) solve the LGS tilt indeterminacy problem, (iii) measure the quadratic wave-front modes from one or more NGSs, or (iv) measure the quadratic wave-front modes from one or more Rayleigh LGSs. Sample numerical calculations

for 8-m telescopes indicate that all of these methods correct for at least some tilt anisoplanatism, although the improvement achieved by method (iii) is fairly modest for this application, with only a single NGS. The signal level requirements for methods (i), (iii), and (iv) do not appear to be unreasonable, although detailed SNR and sky-coverage calculations are beyond the scope of this paper.

The use of so-called hybrid combinations of sodium and Rayleigh guide stars for MCAO has received relatively little attention to date. The hybrid configuration studied here has a number of attractive features, if the complexity of multiple laser systems can be accepted. Sky coverage is maximized, since only a single tip/tilt NGS is required. Image uniformity across the FoV will not suffer with dim NGS, as is the case for approaches requiring multiple- or higher-order NGS WFS. The power requirement for the Rayleigh guide stars is quite low, since the order of the associated wave-front sensors is fairly modest. Further simplifications and advantages can be accrued if the tip/tilt NGS WFS is implemented in the infrared:

- Sky coverage is further improved owing to the sharpening of the NGS image by the AO and the relative frequency of red (class K or M) guide stars,
- The tip/tilt NGS may be placed in the science instrument to measure non-common-path tip/tilt errors such as flexure,
- All wavelengths longer than $\sim 0.6\ \mu$m may be passed through the AO system to the science instrument,
- All wave-front sensors in the AO system have fixed guide-star locations, although the sodium LGS wave-front sensors must be adjustable in focus.

The variety of MCAO system concepts continues to grow and now ranges from complete to absolutely minimal reliance upon NGSs.

APPENDIX A: CONTRIBUTIONS TO TILT ANISOPLANATISM FOR A KOLMOGOROV TURBULENCE SPECTRUM

In this appendix, we evaluate the relative contributions to tilt anisoplanatism associated with the quadratic and cubic Zernike components of turbulence-induced phase distortions. The conventions for the ordering and scaling of the Zernike polynomials are taken from Noll.[11]

By isotropy, we may assume that the angular offset between the two wave fronts in question is in the x direction, i.e. the wave fronts have propagated from the directions $(0, 0)$ and $(\theta, 0)$. The phase distortion ϕ_1 induced in the on-axis wave front by a phase screen at range h from the telescope will be expressed as a sum of orthogonal Zernike polynomials,

$$\phi_1(x, y) = \sum_{i=1}^{\infty} a_i Z_i(x/R, y/R), \tag{A1}$$

where $R = D/2$ is the radius of the telescope aperture. The phase distortion ϕ_2 for the off-axis wave front is then given by

$$\phi_1(x, y) = \sum_{i=1}^{\infty} a_i Z_i[x/R + (h\theta)/R, y/R], \tag{A2}$$

and the difference between the two phase distortions is just

$$\phi_2(x, y) - \phi_1(x, y) = \sum_{i=1}^{\infty} a_i \{Z_i[x/R + (h\theta)/R, y/R] - Z_i(x/R, y/R)\}. \tag{A3}$$

We proceed by evaluating the tilt component of the anisoplanatic wave-front error contributed by each Zernike mode of radial order 2 or 3 and then combining these contributions according to the expected magnitudes of the coefficients a_i for a Kolmogorov turbulence spectrum.

The Zernike focus mode Z_4 is given by the expression

$$Z_4(x/R, y/R) = \sqrt{3}\left[2\left(\frac{x}{R}\right)^2 + 2\left(\frac{y}{R}\right)^2 - 1\right], \tag{A4}$$

and the associated anisoplanatic wave-front error is just

$$a_4\{Z_4[x/R + (h\theta)/R, y/R] - Z_4(x/R, y/R)\} = a_4 4\sqrt{3}\left(\frac{h\theta}{R}\right)\left(\frac{x}{R}\right) + c, \tag{A5}$$

where the constant c is of no interest. Proceeding with the remaining two quadratic Zernike modes,

$$Z_5(x/R, y/R) = 2\sqrt{6}\left(\frac{x}{R}\right)\left(\frac{y}{R}\right), \tag{A6}$$

$$a_5\{Z_5[x/R + (h\theta)/R, y/R] - Z_5(x/R, y/R)] = a_5 2\sqrt{6}\left(\frac{h\theta}{R}\right)\left(\frac{y}{R}\right), \tag{A7}$$

$$Z_6(x/R, y/R) = \sqrt{6}\left[\left(\frac{x}{R}\right)^2 - \left(\frac{y}{R}\right)^2\right], \tag{A8}$$

$$a_6\{Z_6[x/R + (h\theta)/R, y/R] - Z_6(x/R, y/R)\} = a_6\sqrt{6}\left(\frac{h\theta}{R}\right)\left(\frac{x}{R}\right) + c. \tag{A9}$$

The notation σ_2 will denote the rms tilt anisoplanatism introduced by these three Zernike modes. Because the three modes are uncorrelated,[11] the above calculations imply that this quantity may be computed with use of the expression

$$\sigma_2{}^2 = \left(\frac{h\theta}{R}\right)^2 [12\langle a_4{}^2\rangle + 6\langle a_5{}^2\rangle + 6\langle a_6{}^2\rangle], \tag{A10}$$

where the angle brackets denote ensemble averaging over atmospheric turbulence statistics. All three of these modes have an equal variance approximately equal to $0.023(D/r_0)^{5/3}$, where r_0 is the effective coherence diameter of the phase screen.[11] Substituting this value into the last expression gives the result

$$\sigma_2{}^2 = 0.55(D/r_0)^{5/3}\left(\frac{h\theta}{R}\right)^2, \tag{A11}$$

for the mean-square value of the tilt anisoplanatism error associated with quadratic Zernike modes.

An entirely similar computation yields

$$\sigma_3^2 = 1.32(D/r_0)^{5/3}\left(\frac{h\theta}{R}\right)^4, \tag{A12}$$

for the corresponding tilt anisoplanatism contribution from Zernike modes of radial order three. The ratio of the mean-square values of the two contributions is given by

$$\frac{\sigma_3^2}{\sigma_2^2} = \left(\frac{1.55h\theta}{R}\right)^2, \tag{A13}$$

so that the contribution for the quadratic modes will dominate, provided that

$$h\theta \leqslant 0.65R. \tag{A14}$$

This condition is satisfied for many MCAO configurations of interest. For example, the sample problem described in Section 3 has $R = 4$ m, $\theta = 48.6$ arc sec $= 2.36 \times 10^{-4}$ radians at the corner of the square field of view, and an effective altitude $\bar{h} = r_0/(6.88^{3/5}\theta_0) = 3900$ m for a single-layer turbulence profile, yielding the same values of r_0 and θ_0. These parameters yield

$$\bar{h}\theta = 0.23R. \tag{A15}$$

The mean-square magnitude of tilt anisoplanatism induced by the cubic Zernikes is therefore approximately $(0.23/.65)^2 = 0.12$ times the magnitude of the quadratic contribution at the corners of the square FoV. We note that for fixed FoV θ the relative contribution of the cubic modes to tilt anisoplanatism decreases with the square of the telescope aperture diameter. For fourth-order Zernikes the relative contribution will decrease with the fourth power of the aperture diameter, and so on.

Corresponding author Brent L. Ellerbroek can be reached at the address on the title page or by e-mail at bellerbroek@gemini.edu.

REFERENCES

1. J. M. Beckers, "Increasing the size of the isoplanatic patch with multiconjugate adaptive optics," in *ESO Conference on Very Large Telescopes and Their Instrumentation*, M. H. Ulrich, ed. (European Southern Observatory, Garching, Germany, 1988), Vol. 2, pp. 693–703.
2. B. L. Ellerbroek, "First-order performance evaluation of adaptive-optics systems for atmospheric turbulence compensation in extended-field-of-view astronomical telescopes," J. Opt. Soc. Am. A **11**, 783–805 (1994).
3. E. Viard, N. N. Hubin, M. Le Louarn, and A. A. Tokovinin, "Concept and performance of multiple laser guide stars for 8m class telescopes," in *Adaptive Optical Systems Technology*, P. Wizinowich, ed., Proc. SPIE **4007**, 94–105 (2000).
4. R. Flicker, B. L. Ellerbroek, and F. J. Rigaut, "Comparison of multiconjugate adaptive optics configurations and control algorithms for the Gemini-South 8m telescope," in *Adaptive Optical Systems Technology*, P. Wizinowich, ed., Proc. SPIE **4007**, 1032–1043 (2000).
5. F. J. Rigaut, B. L. Ellerbroek, and R. Flicker, "Principles, limitations, and performance of multi-conjugate adaptive optics," in *Adaptive Optical Systems Technology*, P. Wizinowich, ed., Proc. SPIE **4007**, 1022–1031 (2000).
6. R. Ragazzoni, "Adaptive optics for 100m class telescopes: New challenges require new solutions," in *Adaptive Optical Systems Technology*, P. Wizinowich, ed., Proc. SPIE **4007**, 1076–1087 (2000).
7. B. L. Ellerbroek and F. J. Rigaut, "Scaling multiconjugate adaptive optics performance estimates to extremely large telescopes," in *Adaptive Optical Systems Technology*, P. Wizinowich, ed., Proc. SPIE **4007**, 1088–1099 (2000).
8. D. L. Fried, "Artificial-guide-star tilt-anisoplanatism: its magnitude and (limited) amelioration," in *Adaptive Optics*, M. Cullum, ed., Vol. 23 of 1995 OSA Technical Digest Series (Optical Society of America, Washington, D.C., 1995), pp. 363–369.
9. J. Vernin, A. Agabi, R. Avila, M. Azouit, R. Conan, F. Martin, E. Masciadri, L. Sanchez, and A. Ziad, "1998 Gemini site testing campaign: Cerro Pachon and Cerro Tololo," Gemini Document RTP-AO-G0094 (Gemini Observatory, Hilo, Hawaii, 2000).
10. B. L. Ellerbroek and D. W. Tyler, "Adaptive optics sky coverage calculations for the Gemini-North telescope," Proc. Astron. Soc. Pac. **110**, 165–185 (1998).
11. R. J. Noll, "Zernike polynomials and atmospheric turbulence," J. Opt. Soc. Am. **66**, 207–211 (1976).